Proc. Indian Acad. Sci. (Earth Planet. Sci.), Vol. 94, No. 3, November 1985, pp. 269–277.

Transient electromagnetic response due to a pair of horizontal conducting sheets in a loop field

R NAGENDRA, I B RAMAPRASADA RAO and SATYANARAYAN KABRA
Department of Geophysics and Centre of Exploration Geophysics, Osmania University, Hyderabad 500007, India

MS received 10 November 1983; revised 1 February 1985

Abstract. The transient electromagnetic response due to a pair of horizontal conducting sheets induced by a loop field is obtained. The response characteristics in the three different regions (above the upper sheet, between the two sheets and below the lower sheet) are briefly discussed.

In the first and second regions the composite response is characterised by an overburden response asymptote during early times and a target response asymptote during late times. The transition zones are characterised by shoulder-like bends. In the third region, the composite response increases in direct proportion to the induction number, eventually merging with the target response for large values of the induction number.

Keywords. Transient response; conducting sheets; transition zone; overburden.

1. Introduction

Quite often conductive economic mineral deposits occur as fissure veins, bedded type deposits, lenses, etc. in different kinds of relatively less conductive country rocks (Bateman 1958; Swayder 1967; Smironov 1967; Zakharov 1967). Among such country rocks, sedimentary and metamorphic rock types like dolomite, quartzite, phyllite, schist and gneiss are common. A distinctive feature of bedded and lens type mineral deposits is that they can be closely approximated by thin sheet-type conductors.

Usually the conductivities of such ore-bearing rocks vary between 10^{-2} to 10^{-5} seimens, while the conductivities of the ore bodies vary between 10^2–10^4 seimens (Parasnis 1968, 1971; Parkhomenko 1965). In certain frequently encountered geological settings, the ore reserves are covered by conductive soil layers. Usually the conductivities of overburden lie within the range 10^{-3} to 1 seimen (Vingoe 1972).

Thus a thin sheet representing a bedded-type deposit overlain by a less conductive sheet representing the overburden is an important physico-geological situation necessitating a detailed analytical study. Such conductive configurations in spherical and cylindrical geometries were studied by Nagendra *et al* (1980, 1981), for one loop transient measurements in the surface version.

Geophysical investigations in boreholes play a vital role in supplementing the information gathered from surface investigations. Quite often ore bodies missed during the drilling stage can be located in the vicinity by suitable geophysical investigations carried out in the borehole. Especially when the deposit is missed in the lithologs due to limited core recovery or when the bore cuts through a pinched-out region, borehole electromagnetic (EM) investigations offer valuable information in mapping the surrounding conductive inhomogeneities.

In the present paper, the transient electromagnetic response due to a pair of horizontal conducting sheets induced by a loop field (step excitation) is obtained. The response characteristics in the three different regions of the medium (I. above the upper sheet, II. between the two sheets and III. below the lower sheet) are briefly discussed in relation to the single shield (upper sheet), single target (lower sheet) responses. It is hoped that such a study would form the basis for analyzing surface and borehole transient EM data over sheet type bodies.

2. Derivation

Figure 1 illustrates the geometry of a pair of horizontal sheets referred to a cylindrical coordinate system (ρ, θ, z). The two sheets are assumed to be infinitely conducting $(\sigma_{1,2} \to \infty)$ and infinitesimally thin $(T_{1,2} \to 0)$, such that their conductances $(S_1 = \sigma_1 T_1;$ $S_2 = \sigma_2 T_2)$ are finite. The upper sheet is assumed to be located on the surface itself $(z = 0)$, over which the transmitter loop of radius R is laid. The axis of the loop coincides with the z-axis (+ve downward) of the coordinate system. The primary vector potential due to the transmitter loop in the cylindrical co-ordinate system is given by (Makagonov 1969)

$$A_p = \frac{\mu_0 I R}{2} \int_0^\infty J_1(\lambda R) \cdot J_1(\lambda \rho) \cdot \exp(-\lambda z) \cdot \mathrm{d}\lambda \tag{1}$$

In the cylindrical coordinate system (ρ, θ, z), the vector potential $\bar{A}$ satisfies the following wave equation

$$\frac{\partial^2 \bar{A}}{\partial \rho^2} + \frac{1}{\rho}\frac{\partial \bar{A}}{\partial \rho} + \frac{1}{\rho^2}\frac{\partial^2 \bar{A}}{\partial \theta^2} + \frac{\partial^2 \bar{A}}{\partial z^2} - k^2 \bar{A} = 0 \tag{2}$$

where $k = (i\omega\mu\sigma)^{1/2}$ is the wave number.

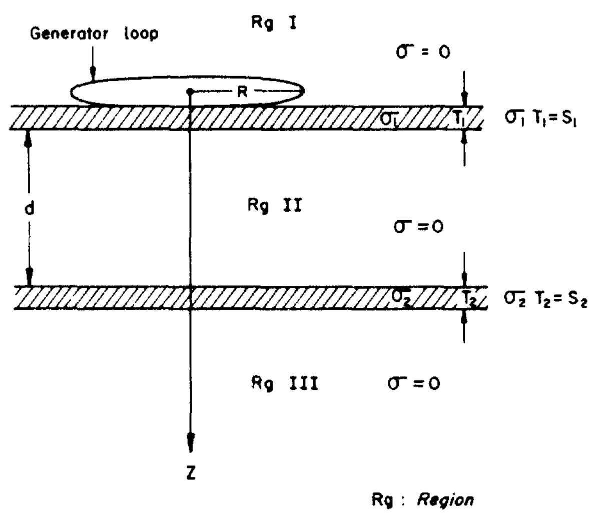

Figure 1. Geometry of a pair of horizontal sheets in a loop field.

In view of the axial symmetry of the chosen model $\bar{A}$ has only a θ component which is independent of θ and can be expressed as,

$$\bar{A} = \hat{a}_\theta \cdot A(r, z) \tag{3}$$

where $\hat{a}_\theta$ is the unit vector in the θ-direction, and $A(r, z)$ is a purely scalar function of r and z, which, for the sake of brevity will be referred to as A.

Converting $\hat{a}_\theta$ into the rectangular coordinate system, we have

$$\hat{a}_\theta = \hat{i}\cos\theta + \hat{j}\sin\theta \tag{4}$$

where $\hat{i}$ and $\hat{j}$ are unit vectors along x and y directions respectively.
Hence

$$\frac{\partial^2 \bar{A}}{\partial \theta^2} = -\hat{a}_\theta \cdot A \tag{5}$$

Making use of (5), (1) in regions not occupied by any conductors ($k = 0$) can be simplified as follows;

$$\frac{\partial^2 A}{\partial \rho^2} + \frac{1}{\rho}\cdot\frac{\partial A}{\partial \rho} - \frac{A}{\rho^2} + \frac{\partial^2 A}{\partial z^2} = 0. \tag{6}$$

Following the procedure of separable variables, solutions of (6) in the regions I, II and III (vide figure 1) can be written as follows, in accordance with the expression for A_p.

$$A_{\mathrm{I}} = M\cdot\{\exp(-\lambda z) + X_0\cdot\exp(\lambda z)\} \tag{7}$$

$$A_{\mathrm{II}} = M\cdot\{X_1\cdot\exp(-\lambda z) + X_2\cdot\exp(\lambda z)\} \tag{8}$$

$$A_{\mathrm{III}} = M\cdot\{X_3\cdot\exp(-\lambda z)\} \tag{9}$$

where $M\{\cdot\} = \dfrac{\mu_0 IR}{2}\displaystyle\int_0^\infty J_1(\lambda R)\cdot J_1(\lambda\rho)\cdot\{\cdot\}\cdot d\lambda$ and X_m $(m = 0, 1, 2, 3)$ are the arbitrary constants.

The term involving the positive exponent of λz is dropped out of (9) in view of the infinity constraints.

Following the boundary conditions (Wait 1969)

$$A_{\mathrm{I}} = A_{\mathrm{II}};\ \frac{\partial A_{\mathrm{I}}}{\partial z} = \frac{\partial A_{\mathrm{II}}}{\partial z} - i\omega\mu_0 S_1\cdot A_{\mathrm{I,II}}|_{z=0} \tag{10}$$

$$A_{\mathrm{II}} = A_{\mathrm{III}};\ \frac{\partial A_{\mathrm{II}}}{\partial z} = \frac{\partial A_{\mathrm{III}}}{\partial z} - i\omega\mu_0 S_2 A_{\mathrm{II,III}}|_{z=d} \tag{11}$$

the X-coefficients could be obtained as

$$X_0 = i\omega C[i\omega(1-p) + 2x(\alpha p + \beta)] \tag{12}$$

$$X_1 = -2x\alpha C[i\omega + 2\beta x] \tag{13}$$

$$X_2 = 2\alpha x p\, i\omega C \tag{14}$$

$$X_3 = -4C\alpha\beta x^2 \tag{15}$$

$$\alpha = (\mu_0 S_1 R)^{-1},\ \beta = (\mu_0 S_2 R)^{-1},\ x = \lambda R$$

where

$$\bar{d} = d/R,\ C = [(\omega - iK_1)(\omega - iK_2)(1-p)]^{-1}$$

$$p = \exp(-2x\bar{d}),\ K_{1,2} = \frac{x}{1-p}(\alpha + \beta \pm D),$$

$$D = [(\alpha - \beta)^2 + 4\alpha\beta p]^{1/2}$$

For evaluating the transient e.m.f. responses in the three different regions it is necessary to obtain inverse Fourier transforms of the X-functions given by

$$x_m(t) = \frac{1}{2\pi}\int_{-\infty}^{\infty} X_m(\omega)\cdot \exp(i\omega t)\cdot d\omega \quad m = 0, 1, 2, 3 \tag{16}$$

Accordingly we can write

$$x_0(t) = \frac{\alpha x}{D}\{(\beta - \alpha + D)\cdot \exp(-K_2 t) - (\beta - \alpha - D)\cdot \exp(-K_1 t)\} \tag{17}$$

$$x_1(t) = \frac{\alpha}{D}\{(2\beta x - K_2)\cdot \exp(-K_2 t) - (2\beta x - K_1)\cdot \exp(-K_1 t)\} \tag{18}$$

$$x_2(t) = \frac{\alpha p}{D}\{K_2 \cdot \exp(-K_2 t) - K_1 \cdot \exp(-K_1 t)\} \tag{19}$$

$$x_3(t) = \frac{2\alpha\beta x}{D}\{\exp(-K_2 t) - \exp(-K_1 t)\} \tag{20}$$

For measurements on the surface ($z = 0$) using the combined loop version, the transient e.m.f. is given by

$$\varepsilon_{\mathrm{I}}(t) = \mu_0 \pi I R \int_0^{\infty} \{J_1(x)\}^2 \cdot x_0(t)\cdot dx \tag{21}$$

Two important limiting expressions of $\varepsilon_{\mathrm{I}}(t)$, viz, single upper sheet response $\varepsilon_{\mathrm{I}1}(t)$, single lower sheet response $\varepsilon_{\mathrm{I}2}(t)$, can be obtained by replacing $x_0(t)$ with $x_{01}(t)$ and $x_{02}(t)$ defined as follows:

$$x_{01}(t) = \operatorname*{Lt}_{\beta \to \infty} x_0(t) = 2\alpha x \cdot \exp(-2\alpha x t) \tag{22}$$

$$x_{02}(t) = \operatorname*{Lt}_{\alpha \to \infty} x_0(t) = 2\beta x \cdot \exp[-2x(\bar{d} + \beta t)] \tag{23}$$

For measurements along the borehole axis with a receiver loop of relatively small radius ($\rho \to 0$) applicable in regions II and III, e.m.f. ε is related to vector potential A as follows:

$$\varepsilon = \operatorname*{Lt}_{\rho \to 0}\left\{\frac{\partial A}{\partial \rho} + \frac{A}{\rho}\right\} \tag{24}$$

Since $J_1(\lambda\rho)$ is the only term involving ρ in the expression for A, it is necessary to evaluate the following limit

$$\operatorname*{Lt}_{\rho \to 0}\left\{\frac{\partial[J_1(\lambda\rho)]}{\partial \rho} + \frac{J_1(\lambda\rho)}{\rho}\right\} = \lambda \tag{25}$$

Accordingly expressions for the transient e.m.f. in regions II and III can be written as

$$\varepsilon_{II}(t) = \frac{\mu_0 I}{2R}\int_0^\infty x\cdot J_1(x)[x_1(t)\cdot \underset{0<\bar{z}<\bar{d}}{\exp}(-x\bar{z})$$

$$+x_2(t)\cdot \exp(x\bar{z})]\cdot \mathrm{d}x \tag{26}$$

$$\varepsilon_{III}(t) = \frac{\mu_0 I}{2R}\int_0^\infty x\cdot J_1(x)\cdot x_3(t)\cdot \underset{\bar{z}>\bar{d}}{\exp}(-x\bar{z})\cdot \mathrm{d}x \tag{27}$$

Where $\bar{z} = z/R$, z being the depth of measurement. The single upper sheet and single lower sheet limiting responses can be obtained for ε_{II} and ε_{III} making use of the following limiting expressions for $x_1(t)$, $x_2(t)$ and $x_3(t)$.

$$x_{11}(t) = \underset{\beta\to\infty}{\mathrm{Lt}}\ x_1(t) = 2\alpha x\cdot \exp(-2\alpha x t) \tag{28}$$

$$x_{12}(t) = \underset{\alpha\to\infty}{\mathrm{Lt}}\ x_1(t) = 0 \tag{29}$$

$$x_{21}(t) = \underset{\beta\to\infty}{\mathrm{Lt}}\ x_2(t) = 0 \tag{30}$$

$$x_{22}(t) = \underset{\alpha\to\infty}{\mathrm{Lt}}\ x_2(t) = 2\beta x\cdot \exp[-2x(\bar{d}+\beta t)] \tag{31}$$

$$x_{31}(t) = \underset{\beta\to\infty}{\mathrm{Lt}}\ x_3(t) = 2\alpha x\cdot \exp(-2\alpha x t) \tag{32}$$

$$x_{32}(t) = \underset{\alpha\to\infty}{\mathrm{Lt}}\ x_3(t) = 2\beta x\cdot \exp(-2\beta x t) \tag{33}$$

3. Numerical solution and results

For the purpose of numerical computation and graphical representation it would be more convenient to rewrite the expressions for ε_I, ε_{II} and ε_{III} [vide (21), (26) and (27)] along with their limiting responses in a non-dimensional parametric form as presented in table 1.

These expressions are utilised for computing the required transient responses. The numerical integration over the variable x is performed using Simpson's rule allowing for an error of $\pm 5\%$ in each case. The results are plotted in figures 2, 3 and 4 for certain values of the model parameters.

4. Discussion

The normalized transient e.m.f. response computed for the combined loop surface version (region I), along with the two limiting responses are plotted as functions of $\tau = \alpha t$ in figure 2 for $S = 100$ and $\bar{d} = \frac{1}{4}, \frac{1}{2}, 1, 2, 4$. It can be observed from this figure that the composite response closely follows the single upper sheet response $\bar{\varepsilon}_1(\tau)$ during

Table 1. Normalized responses.

Region I: Combined loop measurements

$$\bar{\varepsilon}(\tau) = F_1 \varepsilon_{\mathrm{I}}(t)$$

$$= \int_0^\infty \frac{G(x)}{2D^1}\{(\xi - 1 + D^1)\cdot E_2 - (\xi - 1 - D^1)\cdot E_1\}\,\mathrm{d}x$$

$$\bar{\varepsilon}_1(\tau) = \int_0^\infty G(x)\cdot \exp(-2x\tau)\cdot \mathrm{d}x$$

$$\bar{\varepsilon}_2(\tau) = \xi \int_0^\infty \eta G(x)\cdot \exp(-2x\xi\tau)\cdot \mathrm{d}x$$

Region II: $(0 < \bar{z} < \bar{d})$—*Measurements with a receiver loop of negligible radius*

$$\bar{\varepsilon}(\tau) = F_2 \varepsilon_{\mathrm{II}}(t)$$

$$= \int_0^\infty \frac{L(x)}{2D^1}\Big[\{(2\xi x - K_2^1)E_2 - (2\xi x - K_1^1)E_1\}\delta$$

$$+ \{K_2^1 E_2 - K_1^1 E_1\}\frac{\eta}{\delta}\Big]\mathrm{d}x$$

$$\bar{\varepsilon}_1(\tau) = \int_0^\infty \delta x L(x)\cdot \exp(-2x\tau)\cdot \mathrm{d}x$$

$$\bar{\varepsilon}_2(\tau) = \int_0^\infty \xi\eta x \frac{L(x)}{\delta}\cdot \exp(-2x\xi\tau)\,\mathrm{d}x$$

Region III: $(\bar{z} > \bar{d})$—*Measurements with a receiver loop of negligible radius*

$$\bar{\varepsilon}(\xi\tau) = F_3 \cdot \varepsilon_{\mathrm{III}}(t)$$

$$= \int_0^\infty \frac{xL(x)}{D^1}[E_2 - E_1]\delta\,\mathrm{d}x$$

$$\bar{\varepsilon}_2(\xi\tau) = \int_0^\infty xL(x)\delta\cdot \exp(-2x\xi\tau)\,\mathrm{d}x$$

where,

$$F_1 = \frac{S_1}{2\pi I};\quad F_2 = \frac{S_1 R^2}{I};\quad F_3 = \frac{S_2 R^2}{I}$$

$$G(x) = x\cdot[J_1(x)]^2;\quad L(x) = xJ_1(x)$$

$$E_1 = \exp(-K_1^1\tau);\quad E_2 = \exp(-K_2^1\tau)$$

$$\eta = \exp(-2x\bar{d});\ \delta = \exp(-x\bar{z})$$

$$\tau = \alpha t;\ \xi = S_1/S_2$$

$$K_{1,2}^1 = \frac{K_{1,2}}{\alpha};\quad D^1 = \frac{D}{\alpha}$$

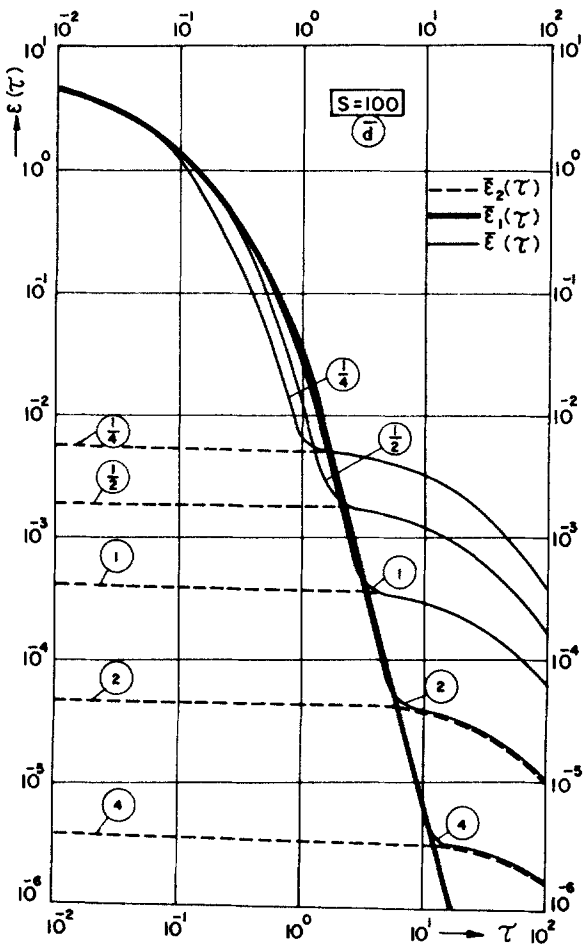

Figure 2. Transient e.m.f. response in region-I (combined loop version).

early times and the single lower sheet response $\bar{\varepsilon}_2(\tau)$ during the late times. Connecting these two time zones is a transition zone characterised by a shoulder-like bend in the composite response. Similar response characteristics were observed over a concentric spherical sheel-shell model by Nagendra *et al* (1980). In view of this, it can be concluded that the gross behaviour of the response is independent of the shield-target geometry.

The composite response function computed for point measurements are plotted in figure 3 for $S = 100$ and $\bar{d} = \frac{1}{4}, \frac{1}{2}, 1, 2, 4$; along with the single upper sheet and single lower sheet limiting functions. The receiver down the bore-hole is assumed to be kept at a depth of 0·24 R. From this figure it can be observed that the composite response characteristics in region II are largely similar to those observed in region I, in relation to their corresponding asymptotic responses. However, an interesting aspect is that the composite response in region II displays an additional shoulder-like bend in the transition zone. This secondary bend decreases gradually in prominence with increasing $\bar{d}$. It appears that this characteristic is mainly related to the placement of the receiver with respect to the target.

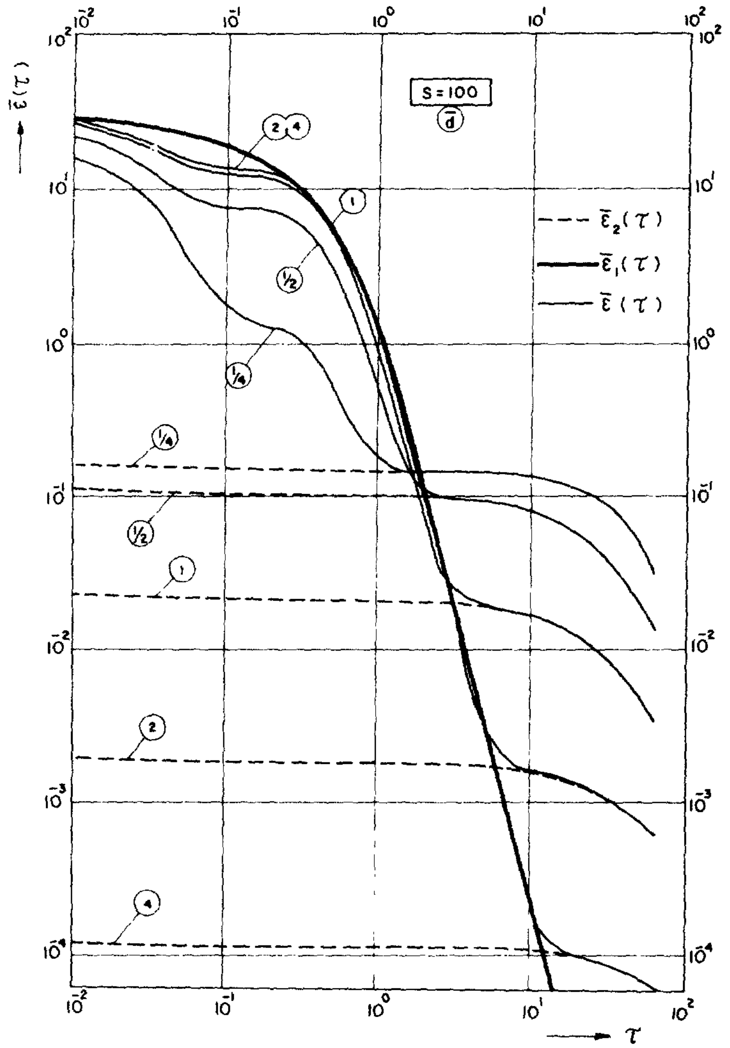

Figure 3. Transient e.m.f. response in region-II (receiver loop of negligible radius).

In figure 4 are plotted the composite response characteristics observed in region III as functions of $\xi\tau = \beta t$, for the following parameters

$$\bar{d} = 0{\cdot}5;\ \bar{z} = 4{\cdot}2;\ S = 1,\ 3{\cdot}16,\ 10,\ 31{\cdot}6,\ 100.$$

The abscissa is chosen as $\xi\tau$ in place of the usual τ for the sake of convenience, since the single upper sheet limiting response is never reached in the composite response characteristic. The curve labelled $S = \infty$, corresponds to the single lower sheet limiting response.

It can be observed from figure 4 that the composite response increases in magnitude in direct proportion to $\xi\tau$, during early times, eventually merging with the single lower sheet limiting response. The merger takes place at much earlier times for larger S values as expected.

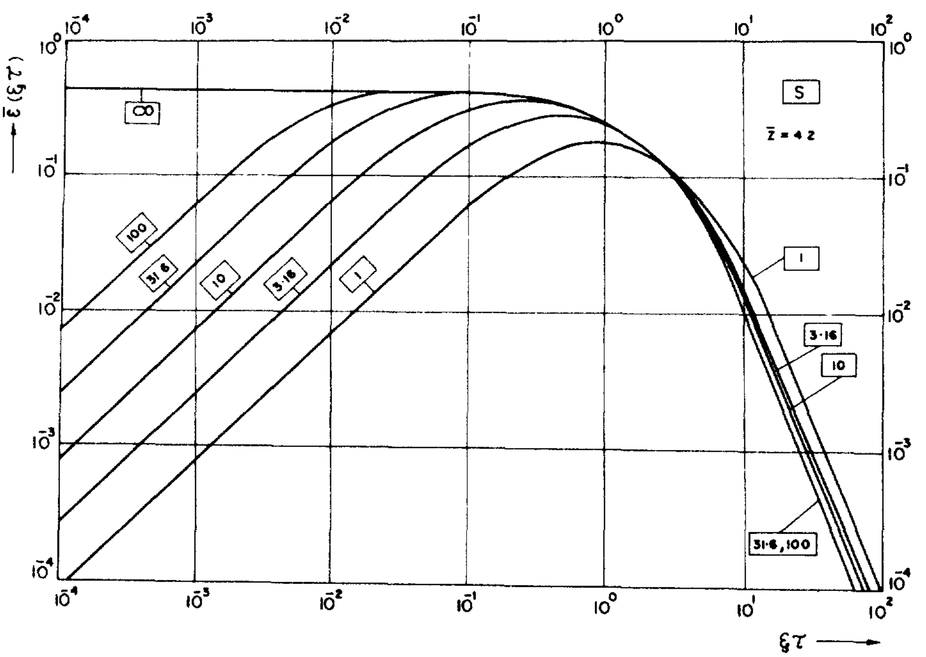

Figure 4. Transient e.m.f. response in region-III (receiver loop of negligible radius).

References

Bateman A M 1958 *Economic mineral deposits* (Bombay: Asia Publishing House) p. 111

Makagonov P P 1969 *IZV. Akad. Sci. USSR (in Russian)* **3** 57

Nagendra R, Ramaprasada Rao I B and Bhimasankaram V S 1980 *Geophys. Prospect.* **28** 269

Nagendra R, Ramaprasada Rao I B and Bhimasankaram V S 1981 *Bull.-Aust. Soc. Explor. Geophys.* **12** 29

Parasnis D S 1968 ABEM Geophysical memorandum 1/68

Parasnis D S 1971 ABEM Geophysical memorandum 4/71

Parkhomenko E I 1965 *Electrical properties of rocks* (in Russian) (Moscow: Nauka) p. 73

Smironov V I 1967 *Econ. Geol. Monogr.* **3** 219

Swayder F G 1967 *Econ. Geol. Monogr.* **3** 1

Vingoe P 1972 ABEM Geophysical memorandum 5/72

Wait J R 1969 *Geophysics* **34** 753

Zakharov E E 1967 *Econ. Geol. Monogr.* **3** 221